



Open Archive TOULOUSE Archive Ouverte (OATAO)

OATAO is an open access repository that collects the work of Toulouse researchers and makes it freely available over the web where possible.

This is an author-deposited version published in : <http://oatao.univ-toulouse.fr/>
Eprints ID : 10504

To cite this version : Chauvet, Fabien and Geoffroy, Sandrine and Hamouni, Abdelkrim and Prat, Marc and Gué, Anne-Marie and Joseph, Pierre Nanobubbles and gas dynamics during capillary filling of nanochannels. (2012) In: The 16th International Conference on Miniaturized Systems for Chemistry and Life Sciences, 28 October 2012 - 01 November 2012 (Japan).

Any correspondence concerning this service should be sent to the repository administrator: staff-oatao@listes-diff.inp-toulouse.fr

NANOBUBBLES AND GAS DYNAMICS DURING CAPILLARY FILLING OF NANOCHANNELS

Fabien Chauvet^{1,2}, Sandrine Geoffroy³, Abdelkrim Hamoumi^{1,2}, Marc Prat⁴, Anne-Marie Gué^{1,2} and Pierre Joseph^{1,2}

¹CNRS, LAAS, 7 avenue du colonel Roche, F-31400 Toulouse, France

²Univ de Toulouse, LAAS, F-31400 Toulouse, France

³ICA, INSA ; Univ de Toulouse, 135 avenue de Rangueil, F31400 Toulouse, France

⁴CNRS, IMFT ; Univ de Toulouse, 2 Allée du Professeur Camille Soula ; F31400 Toulouse, France

ABSTRACT

This paper focuses on capillary filling at the nanoscale where deviations to the Washburn's classical theory are observed. Imbibition experiments in microfabricated silicon-glass nanochannels with low aspect ratio (width \gg depth and depths going from 400 nm down to 20 nm) are performed for several liquids. In all cases, as predicted by the Washburn's law, liquid invasion front location evolves as the square root of time. However, filling kinetics slowdown compared to the Washburn's law is measured in nanochannels for depths below ~ 100 nm. Furthermore, below a liquid-dependent depth threshold, we observe spontaneous bubbles formation behind the advancing meniscus. Bubbles dynamics (formation conditions and lifetime) are analyzed thanks to our experimental data involving several liquids and nanochannels depths. Viscous resistance induced by the bubbles presence is estimated using an effective medium approach. Conjointly, gas flow ahead of the advancing meniscus is modeled considering the gas as viscous and compressible. Influence of these effects on the filling kinetics is discussed.

KEYWORDS

Capillary filling, nanochannels, nanofluidics

INTRODUCTION

At macro and micro-scales, Washburn's law [1] predicts that the filling length (liquid front location) evolves as the square root of time ($t^{1/2}$) and it is generally verified quantitatively. At the nanoscale (typically below ~ 100 nm), filling length continues to evolve as $t^{1/2}$ but deviations are usually observed such as filling kinetics slowdown [2-3] and bubbles formation behind the meniscus [3-4]. Studying these deviations to the classical macroscopic behavior at the nanoscale should allow better understanding and control of nanofluidic flows which play an important role in various fields such as nano-emulsions production [5] for instance.

Even if several works have investigated specific processes such as electroviscous effect (for water) [6] or bubbles induced hydrodynamic resistance [4], number of phenomena able to explain the filling kinetics slowdown remain to be analyzed. In this context, we focus on the poorly explored role of gas during nanochannels capillary filling. First, bubbles generation conditions and lifetime are measured for different liquids (water, ethanol, isopropanol and a silicone oil) and nanochannels geometries: $20 \text{ nm} < \text{depth} < 400 \text{ nm}$, $200 \text{ }\mu\text{m} < \text{length} < 5 \text{ mm}$ and $3 \text{ }\mu\text{m} < \text{width} < 10 \text{ }\mu\text{m}$. As bubbles can slowdown the liquid flow, viscous resistance induced by their presence is estimated using an effective medium approach. Second, the gas flow in front of the advancing meniscus is modeled assuming it as viscous and compressible.

EXPERIMENTS

Nanochannels are realized by standard clean-room fabrication. Lateral dimension of the channels are designed on a photomask: width is varied between $3 \text{ }\mu\text{m}$ and $10 \text{ }\mu\text{m}$, and length between $200 \text{ }\mu\text{m}$ and 5 mm , as shown in Figure 1. Nanochannels are etched in silicon by reactive ion etching with conditions adapted to slow smooth etching (etching rate is around $10 \text{ nm}\cdot\text{min}^{-1}$) and the obtained peak-to-peak roughness, measured by Atomic Force Microscopy (AFM), is below 1 nm on a $2.5 \text{ }\mu\text{m}$ line. Microchannels ($10 \text{ }\mu\text{m}$ deep, $200 \text{ }\mu\text{m}$ wide) are also dry etched; they provide a fast and reproducible arrival of the liquid during the capillary filling experiments. Holes are drilled by sand blasting at microchannels ends. Sealing of the silicon wafer to a glass substrate is ensured by anodic bonding. Bonding parameters (temperature $T=370^\circ\text{C}$, Voltage $V=250\text{V}$, limiting current 4mA) are chosen to minimize channel collapse. Contact angles are measured just before the bonding step by drop deposition method (Digidrop apparatus). Full wetting is obtained for the different liquids, so the contact angle is supposed to be lower than 5° , the minimum angle that can reasonably be measured by this method. Channel depth is varied between 20 nm and 400 nm . It is measured by a calibrated AFM. The values are consistent with the ones obtained on test zones of width much larger than those of the nanochannels by a mechanical profilometer and an optical interferometry profilometer, with a maximum deviation of a few percents.

Filling kinetics experiments are realized on an inverted microscope (Zeiss Axio Observer D1), with $10\times$ objective, and a high speed camera (Photron Fastcam SA3). Imbibition is characterized for deionized water (clean-room quality, $18 \text{ M}\Omega\cdot\text{cm}$), ethanol, isopropanol (electronic grade), and silicone oil (Siliconöl M5, Carl Roth). Standard reflection illumination with a halogen lamp gives a good contrast between dry and wetted zone for depths down to 20 nm . Devices are stored in an oven at 200°C for 30 min just before the experiments. The chip is inserted in a Teflon holder and liquid arrival is realized by deposition of a $5 \text{ }\mu\text{L}$ droplet. The temperature is measured for each experiment; its value is in the range $21\text{-}26^\circ\text{C}$. Relative hygrometry is around 45% .

CAPILLARY FILLING SLOWDOWN AND BUBBLES DYNAMICS

Our results on imbibition rates are compatible with published data [2-4]: $t^{1/2}$ evolution of meniscus position but the filling rate is significantly lower than Washburn's prediction (Figure 2). The relative slowdown shows no dependence with channel width (from 3 to 10 μm) and length (from 200 μm to 5 mm), within a few percents.

As reported earlier, we detect trapping of bubbles for the thinnest channels. We have systematically investigated this process: we observe a threshold in nanochannel depth for different solvents (water, ethanol and silicone oil). This threshold is reached first for water, then for ethanol; and bubbles appear for oil only in the narrower devices (Figure 3). The precise physical mechanism responsible for bubble trapping is still unclear, but our observations suggest that it could be related to contact line pinning by chemical or topological defects. As a matter of fact, even though we measure a zero contact angle just before bonding the devices at a macroscopic scale, wetting on silicon oxide surface (glass or silicon native oxide) is better for silicone oil (the spreading parameter is higher) than for ethanol and for water, so that water (and to a lower extent ethanol) should be more subject to pinning than the oil. This point deserves a specific study.

Bubbles are actually trapped: they are not convected by the flow, but their volume decreases during time until their final collapse. This dynamics should be governed first by compression, due to the local liquid pressure increase, and then, once the inside bubble pressure is sufficiently high, gas dissolution should lead to the bubble disappearance. Consequently, relative durations of these regimes are expected to depend strongly on the solubility of the gas in the liquid. Indeed, our experimental results, involving different liquids for which air solubilities are different, allow validating this proposed mechanism.

Stagnant bubbles act as obstacles in the liquid flow and then they induce a viscous resistance which was proposed to explain the observed capillary filling slowdown. This effect is estimated using an effective medium approach (Brinkman's approximation) allowing computing the permeability of a model Hele-Shaw channel (low aspect ratio channel) including a regular arrangement of bubbles. Surprisingly, for nanochannels depths < 100 nm, the permeability computed is very close to the permeability of a bubbles-free Hele-Shaw channel suggesting that bubbles presence is not responsible of the capillary filling slowdown. Actually, viscous resistance induced by the presence of bubbles spaced by micrometric sizes is negligible compared to the viscous resistance of the very confined nanochannels.

GAS DYNAMICS

Gas flow ahead of the advancing meniscus can also induce a resistance and then slowdown the liquid flow. In order to investigate the influence of this effect during capillary filling of nanochannels, we have performed a modeling of the transient gas flow taking into account its viscosity and its compressibility. Derived conservation equations have to be solved numerically on a shrinking domain. For the test case of capillary filling in 50 nm depth and 1 mm long nanochannel, we find a gas over-pressure in front of the meniscus of ~ 1 bar (relative to the atmosphere), see Figure 4. Amplitude and relative duration of the gas over-pressure at the meniscus increase when the nanochannel depth is decreased, see Figure 4. We see that a significant pressurization of the gas occurs during capillary filling of nanochannels showing that gas compressibility has to be taken into account to correctly model this system. However, over-pressures computed are not sufficiently high to explain the experimentally observed capillary filling slowdown. Indeed, gas over-pressure has to be compared to the liquid pressure difference, i.e. the capillary pressure jump, which is much higher at these nano-scales (72 bars for water in a 20 nm depth nanochannel). Additional computations have been performed taking into account presence of precursor liquid films covering channel walls. In the latter case, for sufficiently thick liquid films, a capillary filling slowdown compatible with experiments has been computed.

CONCLUSION

We have analyzed the capillary filling of simple fluids in low aspect ratio nanochannels. Capillary filling experiments have been performed in silicon-glass microfabricated nanochannels. In agreement with existing literature, we found a significant slowdown compared to the classical Washburn's law and we observed spontaneous bubbles formation for nanochannels depths < 100 nm. We focus on the effect of the bubbles presence and on the effect of the gas pressurization in order to estimate their influence on the particular capillary filling kinetics experimentally measured. None of these effects can explain the measured slowdown except for the pressurization effect if precursor liquid films are present on nanochannel walls.

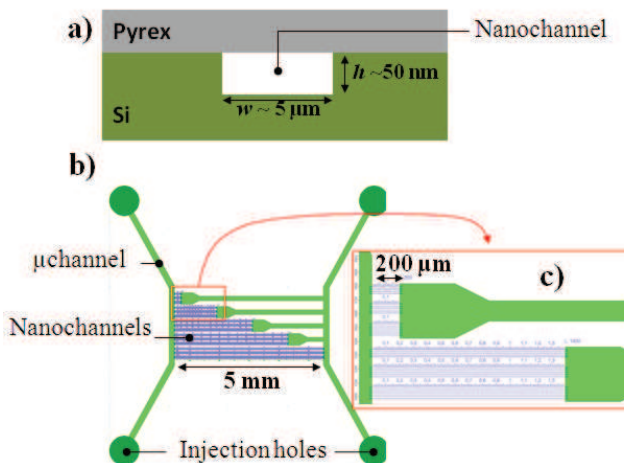


Figure 1: (a) Si-Pyrex nanochannel section view. (b) Architecture of a typical chip used consisting of nanoslits (in violet) with different widths and lengths; self capillary filling of microchannel (in green) allows to bring liquid in nanochannels. (c) Nanochannels closer view: for each length, 3 nanoslits widths family (3, 7 and 10 μm) are etched in Silicon.

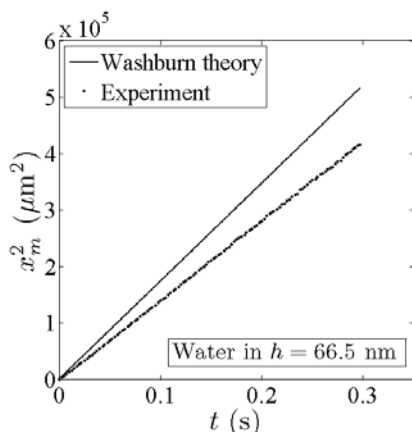


Figure 2: capillary filling kinetics of deionized water in a 66.5 nm deep nanoslit. x_m : position of the liquid front from the nanochannel entrance. Points: experiment; line: Washburn's theory, $x_m^2 = At$. Measured value of A is 20% lower than the theoretical one.

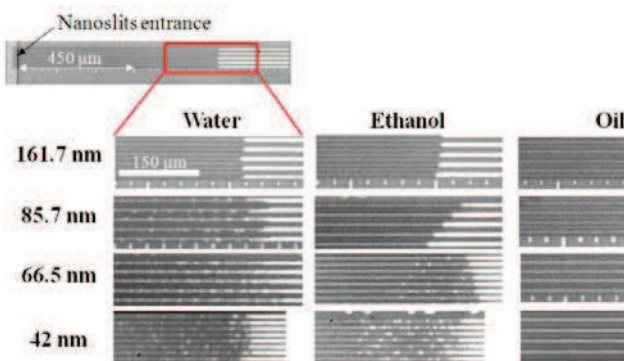


Figure 3: snapshots taken during capillary filling of water, ethanol and one silicone oil for several nanoslits depths. For all the images, the distance between liquid front and the nanoslits entrance is $\sim 750 \mu\text{m}$.

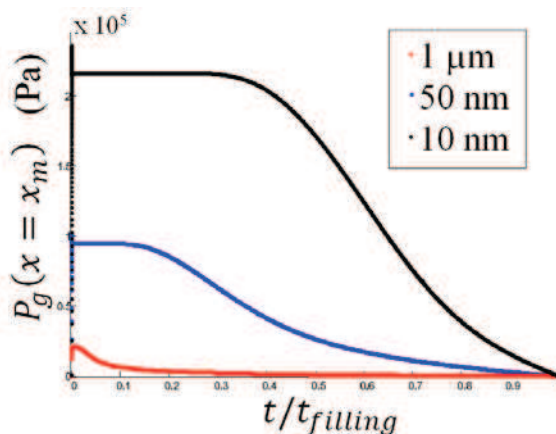


Figure 4: numerically computed over-pressure of air (relative to the atmosphere) ahead the advancing meniscus as a function of the dimensionless time (divided by the filling time) for 3 nanoslits depths.

REFERENCES

- [1] E. W. Washburn, *The dynamics of capillary flow*, Physical Review, 17, 273–283 (1921)
- [2] A. Hibara, T. Saito, H. Kim, M. Tokeshi, T. Ooi, M. Nakao and T. Kitamori, *Analytical Chemistry*, *Nanochannels on a Fused-Silica Microchip and Liquid Properties Investigation by Time-Resolved Fluorescence Measurements*, 74, 6170-6176 (2002)
- [3] A. Han, G. Mondin, N. G. Hegelbach, N. F. de Rooij and U. Staufer, *Filling kinetics of liquids in nanochannels as narrow as 27 nm by capillary force*, Journal of Colloid and Interface Science, 293, 151–157 (2006)
- [4] L. H. Thamdrup, F. Persson, H. Bruus and A. Kristensen, *Experimental investigation of bubble formation during capillary filling of SiO₂ nanochannels*, Applied Physics Letters, 91, 163505 (2007)
- [5] L. Shui, A. van den Berg and J. C. T. Eijkel, *Scalable attoliter monodisperse droplet formation using multiphase nano-microfluidics*, Microfluid Nanofluid, 11, 87–92 (2011)
- [6] N. R. Tas, J. Haneveld, H. V. Jansen, M. Elwenspoek and A. van den Berg, *Capillary filling speed of water in nanochannels*, Applied Physics Letters, 85, 15 (2004)

ACKNOWLEDGEMENTS

We acknowledge CNRS and French National Research Agency for funding (Smart-US program).

CONTACT

Pierre Joseph
 CNRS, LAAS; Univ de Toulouse, 7 avenue du colonel
 Roche F31400 Toulouse, France
 pjoseph@laas.fr